

# Molecular Hydrogen Formation from Proximal Glycol Pairs on TiO<sub>2</sub>(110)

Long Chen, Zhenjun Li,<sup>†</sup> R. Scott Smith, Bruce D. Kay, and Zdenek Dohnálek\*

Fundamental and Computational Sciences Directorate and Institute for Integrated Catalysis, Pacific Northwest National Laboratory, P.O. Box 999, Richland, Washington 99352, United States

**S** Supporting Information

**ABSTRACT:** Understanding hydrogen formation on TiO<sub>2</sub> surfaces is of great importance, as it could provide fundamental insight into water splitting for hydrogen production using solar energy. In this work, hydrogen formation from glycols having different numbers of methyl end-groups has been studied using temperature-programmed desorption on reduced, hydroxylated, and oxidized rutile TiO<sub>2</sub>(110) surfaces. The results from OD-labeled glycols demonstrate that gas-phase molecular hydrogen originates exclusively from glycol hydroxyl groups. The yield is controlled by a combination of glycol coverage, steric hindrance, TiO<sub>2</sub>(110) order, and the amount of subsurface charge. Combined, these results show that proximal pairs of hydroxyl-aligned glycol molecules and subsurface charge are required to maximize the yield of this redox reaction. These findings highlight the importance of geometric and electronic effects in hydrogen formation from adsorbates on TiO<sub>2</sub>(110).

The technological importance of TiO<sub>2</sub> has driven cutting-edge research with the aim of understanding the elementary steps that underlie catalytic and photocatalytic reactions on this material.<sup>1–5</sup> In this context hydrogen, as a promising source of clean, renewable, and environmentally friendly energy, is of great interest.<sup>2,6–8</sup> As such, understanding the factors that control its formation in the thermal and photocatalytic conversion of water and organics is of critical importance. While a significant effort has been devoted to this subject, the mechanism of hydrogen formation on TiO<sub>2</sub> is far from understood.

For catalytic and photocatalytic studies in particular, the most stable TiO<sub>2</sub> surface, rutile TiO<sub>2</sub>(110), has served as a prototypical model.<sup>4,5</sup> When stoichiometric or slightly reduced, the surface is unreconstructed and composed of alternating 5-fold-coordinated Ti<sup>4+</sup> (Ti<sub>5c</sub>) and bridging oxygen (O<sub>b</sub>) rows. A small fraction of bridging oxygen vacancy defects (V<sub>O</sub>'s) that form as a consequence of TiO<sub>2</sub> bulk reduction during ultrahigh vacuum (UHV) preparation, play an important role in determining the surface reactivity of TiO<sub>2</sub>(110).<sup>1,4</sup>

Water and alcohols have been thoroughly investigated on TiO<sub>2</sub>(110) due to their importance as models in studies of photocatalytic water splitting and photo-oxidation of organic contaminants.<sup>1–5</sup> Both water and alcohol molecules initially dissociate at a V<sub>O</sub> site filling it with a hydroxy (HO<sub>b</sub>) and/or alkoxy group, respectively, and splitting hydrogen that forms

another HO<sub>b</sub> group.<sup>9–13</sup> Upon heating to ~500 K, the resulting HO<sub>b</sub>'s recombine with another HO<sub>b</sub> or an alkoxy to produce a water or an alcohol molecule, respectively.<sup>14–18</sup> For alcohols, the majority of alkoxy species (except for methanol which recombinatively desorbs) undergo dehydration to alkenes and water.<sup>15–18</sup> As a consequence, molecular hydrogen desorption from alcohols and water on TiO<sub>2</sub>(110) has not been generally observed.<sup>15–21</sup> In line with these observations, theoretical calculations demonstrate that the kinetic barrier for H<sub>2</sub> recombinative desorption from HO<sub>b</sub> sites on TiO<sub>2</sub>(110) is considerably higher than the barrier for water formation.<sup>20,21</sup> However, in a recent temperature-programmed desorption (TPD) study,<sup>22</sup> Xu *et al.* reported that D<sub>2</sub> is formed as a minor product via thermal recombination of the D atoms on O<sub>b</sub> sites from photocatalysis of methanol. Interestingly, hydrogen desorption between 375 and 500 K was also observed in our recent study of ethylene glycol (EG) reactions on TiO<sub>2</sub>(110).<sup>23</sup>

Molecular hydrogen evolution from EG on TiO<sub>2</sub>(110) was first observed in a study of ethanol, *n*- and 2-propanol, EG, and diethyl ether via TPD and X-ray photoelectron spectroscopy (XPS).<sup>24</sup> Subsequent detailed quantitative investigations with different isotopes (i.e., HO(CH<sub>2</sub>)<sub>2</sub>OH, DO(CH<sub>2</sub>)<sub>2</sub>OD, and HO(CD<sub>2</sub>)<sub>2</sub>OH) demonstrated that the observed hydrogen originates solely from hydroxyl groups and that high EG coverages are required for its formation.<sup>23</sup> While at low coverages, ethylene and water were identified as the only products, at saturation coverage both ethylene + water and acetaldehyde + hydrogen were observed. Total product yield of carbon-containing products at saturation coverage was determined to be ~0.5 monolayer (ML), which clearly shows that the reactions proceed not only at V<sub>O</sub> defect sites but also on the Ti<sub>5c</sub> rows.

In this study, we systematically investigate hydrogen formation from a series of glycols with different steric constraints on differently prepared TiO<sub>2</sub>(110) surfaces in order to further understand hydrogen formation from glycols, and polyols in general. We find that hydrogen formation is dramatically attenuated for glycols with methyl end-groups shielding the hydroxyl functional groups. Further, hydrogen formation is not observed on disordered or oxidized TiO<sub>2</sub>(110). These results suggest that on TiO<sub>2</sub>(110), pairs of aligned glycol molecules with hydroxyl groups in close proximity, together with subsurface charge are required to carry out this redox reaction.

Received: January 28, 2014

Published: April 4, 2014

The experiments were carried out in a UHV molecular beam surface scattering apparatus (base pressure  $< 7 \times 10^{-11}$  Torr) described previously.<sup>16,25</sup> A rutile  $\text{TiO}_2(110)$  crystal ( $10 \times 10 \times 1$  mm<sup>3</sup>, Princeton Scientific) was cleaned by cycles of  $\text{Ne}^+$  sputtering and annealing to 850–900 K in UHV until impurities were undetectable in Auger electron spectra. The surface prepared in this way (referred to as  $r\text{-TiO}_2(110)$ ) contained  $\sim 5\%$   $\text{V}_\text{O}$  defects as determined by  $\text{H}_2\text{O}$  TPD.<sup>14,26</sup> Additionally, hydroxylated ( $h\text{-TiO}_2(110)$ ) and oxidized ( $o\text{-TiO}_2(110)$ ) surfaces were prepared by exposing  $r\text{-TiO}_2(110)$  to  $\text{D}_2\text{O}$  at 400 K, and to  $\text{O}_2$  at 70 K, followed by annealing to 300 K, respectively.<sup>27,28</sup> All glycols (ethylene glycol, 1,2- and 1,3-propylene glycols, 2,3-butylene glycol, 2,3-dimethyl-2,3-butylene glycol) used in this study were obtained from Sigma-Aldrich and transferred into flasks with baked molecular sieves. The glycols were purified by pumping at room temperature, and their temperature during the dose was stabilized in a water bath. The glycols were dosed onto the various  $\text{TiO}_2(110)$  surfaces using an effusive molecular beam. TPD measurements (ramp rate of 1 K/s) were performed using a quadrupole mass spectrometer (UTI).

To unambiguously determine the origin of hydrogen (O–H vs C–H), we employ OD-labeled glycols and monitor the  $\text{D}_2$  signal during the TPD experiments. Since not all OD-labeled glycols are commercially available we prepared them directly on  $\text{TiO}_2(110)$  using an H/D exchange procedure as described in the Supporting Information (SI). The viability of this procedure has been confirmed by comparing the TPD spectra from the isotopically exchanged 1,2-propylene glycol (1,2-PG) with those of commercially available OD-labeled 1,2-PG (Figure S1, SI). The use of OD-labeled glycols further allows us to overcome the experimental difficulties associated with high  $\text{H}_2$  background during TPD due to  $\text{H}_2$  desorption from a closed-cycle He-cryostat cooled manipulator.<sup>23</sup>

Figure 1a shows the coverage-dependent  $\text{D}_2$  TPD spectra from OD-labeled ethylene glycol ( $\text{DO}(\text{CH}_2)_2\text{OD}$ ), 1,3-propylene glycol ( $\text{DO}(\text{CH}_2)_3\text{OD}$ ), 1,2-propylene glycol ( $\text{DOCH}_2\text{CH}(\text{CH}_3)\text{OD}$ ), 2,3-butylene glycol ( $\text{DOCH}(\text{CH}_3)\text{CH}(\text{CH}_3)\text{OD}$ ), and 2,3-dimethyl-2,3-butylene glycol ( $\text{DOC}(\text{CH}_3)_2\text{C}(\text{CH}_3)_2\text{OD}$ ) on  $r\text{-TiO}_2(110)$ . Other products include water and a broad range of carbon-containing species. While the discussion of the carbon-containing products for all employed glycols is beyond the scope of this report, generally alkenes are observed at low coverages, and both alkenes and aldehydes/ketones are seen at high coverages. For EG, all the products and their coverage dependences were discussed in detail in our prior publication<sup>23</sup> and are also summarized in Figure S2 in SI. Further, since  $\text{D}_2$  desorption occurs at lower temperatures than desorption of any carbon-containing products (see data for EG<sup>23</sup> in Figure S2, SI), we believe that  $\text{D}_2$  formation is largely decoupled from the formation of carbon-containing products at higher temperatures.

The selected sequence of glycol molecules allows us to explore how the methyl end-groups that surround the hydroxyl functional groups affect  $\text{D}_2$  formation. Figure 1a shows that for each glycol molecule. With the exception of 2,3-dimethyl-2,3-butylene glycol, the amount of desorbing  $\text{D}_2$  is strongly dependent on the coverage. While at low coverages ( $< 0.25$  ML),  $\text{D}_2$  is practically absent, as the coverage increases to 0.5–1 ML,  $\text{D}_2$  is observed for all glycols except 2,3-dimethyl-2,3-butylene glycol. As further discussed below, the absence of  $\text{D}_2$  for 2,3-dimethyl-2,3-butylene glycol throughout the whole coverage range is a result of the steric hindrance introduced by

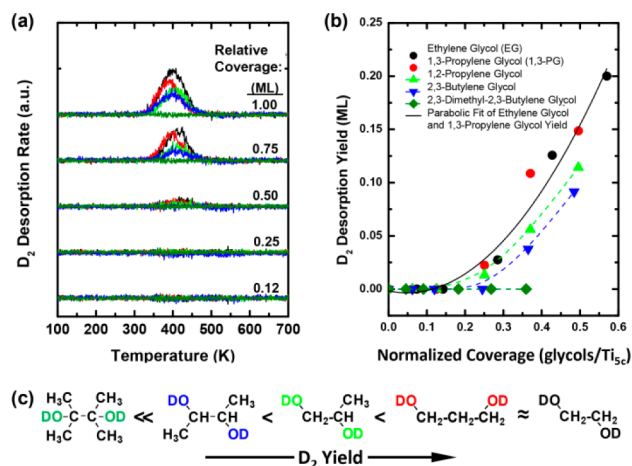


**Figure 1.** (a) Coverage-dependent TPD spectra of  $\text{D}_2$  ( $m/z = 4$  ( $\text{D}_2^+$ )) following ethylene glycol (black), 1,3-propylene glycol (red), 1,2-propylene glycol (green), 2,3-butylene glycol (blue), and 2,3-dimethyl-2,3-butylene glycol (olive) doses listed in the figure. For comparison, all OD-labeled glycols used in these experiments were prepared directly on  $\text{TiO}_2(110)$  using an H/D exchange procedure described in SI. Saturation coverages (defined as 1 monolayer (ML)) correspond to the glycol exposures that saturate the high temperature TPD peak from the parent glycol molecules (see Figure S3, SI). (b) Coverage-dependent  $\text{D}_2$  desorption yields determined from (a). To obtain normalized glycol coverages (glycol molecules per  $\text{Ti}_{5c}$  site), we normalized each coverage in (a) using the corresponding C 1s XPS peak areas of the C–OH moieties (see Figures S4 and S5 in SI for details) and employed the known saturation coverage of methanol (0.77 methanol/ $\text{Ti}_{5c}$ ) as a reference.<sup>29</sup> (c) Schematic structures of studied glycols in the order of increasing  $\text{D}_2$  yield.

four  $-\text{CH}_3$  end-groups that surround the hydroxyl functional groups. The  $\text{D}_2$  desorption peaks for the remaining four glycols extend from 375 to 500 K with the peak area increasing and peak maximum shifting slightly to lower temperature with increasing initial glycol coverage. The fact that the desorption temperatures are the same for all the glycols indicates that the rate limiting step is identical. As the coverage of glycols on  $\text{Ti}_{5c}$  rows reaches saturation,  $\text{D}_2$  desorption saturates as well (spectra above saturation coverages not shown).

The integrated  $\text{D}_2$  yields from Figure 1a are displayed as a function of normalized glycol coverage in Figure 1b. To compare the relative  $\text{D}_2$  yield for the same number of adsorbed glycol molecules, we normalized each glycol coverage from (a) using the corresponding C 1s XPS peak area for the C–OH moieties (see Figures S4 and S5 in SI for details) and the known saturation coverage of methanol (0.77 methanol/ $\text{Ti}_{5c}$ ).<sup>29</sup> As expected, the normalized saturation coverages decrease with increasing number of methyl end-groups in the glycols, and the normalized saturation EG coverage of 0.57 EG/ $\text{Ti}_{5c}$  is in reasonable agreement with the saturation coverage of 0.43 EG/ $\text{Ti}_{5c}$  determined previously.<sup>23</sup> Further, our previous EG study has shown that at saturation coverage, one  $\text{D}_2$  is obtained on average per every two adsorbed EG molecules.<sup>23</sup> This  $\text{D}_2$  yield is used to calibrate the absolute  $\text{D}_2$  yields for other glycols in Figure 1b.

The integrated yields for all the glycols exhibit similar, superlinear dependences on coverage. In our previous study of EG we noted that neighboring  $\text{Ti}_{5c}$ -bound EG molecules may be required for the  $\text{D}_2$  formation.<sup>23</sup> For spatially random adsorption on the  $\text{Ti}_{5c}$  rows, the coverage of EG pairs and hence  $\text{D}_2$  yield should scale with the coverage squared. To see

whether this is indeed the case we fit the data for EG to a parabolic functional form. Generally a good fit is obtained as illustrated by the solid black line shown in Figure 1b.

The quadratic yield dependence suggests that D<sub>2</sub> formation requires the proximal location of OD from aligned glycols. With the above picture in mind, the D<sub>2</sub> yields from different glycols can be compared (Figure 1c). The simplest comparison can be made for ethylene glycol and 1,3-propylene glycol. As both OD groups are primary in both molecules, a similar yield can be expected. Indeed, the D<sub>2</sub> desorption yields from ethylene glycol and 1,3-propylene glycols are identical within the uncertainty of the measurement. Further, the trends in D<sub>2</sub> yield can be evaluated as a function of increasing steric hindrance introduced by the –CH<sub>3</sub> end-groups by following the sequence of ethylene glycol analogues, i.e., 1,2-propylene glycol (–CH<sub>3</sub> at one end), 2,3-butylene glycol (–CH<sub>3</sub> on both ends), and 2,3-dimethyl 2,3-butylene glycol (two –CH<sub>3</sub> on both ends). This is schematically illustrated in Figure 2 for the case of 1,2-PG

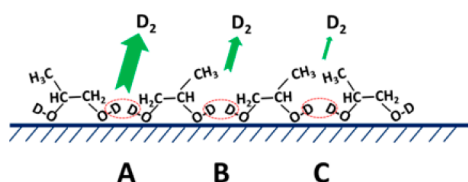


**Figure 2.** Three possible configurations of 1,2-propylene glycol molecular pairs on TiO<sub>2</sub>(110). From A to C, the steric hindrance increases, while D<sub>2</sub> formation probability decreases.

where three possible paired configurations can be envisioned. As suggested by the experimental data (Figure 1), –CH<sub>3</sub> end-groups decrease the probability of an efficient interaction between the hydroxyl groups of neighboring glycol molecules and reduce the D<sub>2</sub> yield. Accordingly, the saturation D<sub>2</sub> yield decreases from 0.20 ML for ethylene glycol to 0.11, 0.09, and finally to 0 for 1,2-propylene glycol, 2,3-butylene glycol, and 2,3-dimethyl 2,3-butylene glycol, respectively. The observed glycol dependences indicate that D<sub>2</sub> is formed directly from two neighboring OD species rather than being a result of recombination of deuterium diffusing on Ti<sub>5c</sub> rows.

To further test the hypothesis that D<sub>2</sub> is being formed from pairs of neighboring glycol molecules bound on Ti<sub>5c</sub> rows, we examined D<sub>2</sub> formation on TiO<sub>2</sub>(110) disordered by gentle sputtering (~2 ML of Ne<sup>+</sup>). In accord with the steric hindrance arguments presented above, disordered TiO<sub>2</sub>(110) is expected to prevent the formation of proximal pairs of hydroxyl groups from aligned glycol molecules. Figure 3 shows the effect of Ne<sup>+</sup>-sputtering on D<sub>2</sub> formation on the surfaces saturated with EG and 1,2-PG. Consistent with the expectations, D<sub>2</sub> is almost completely suppressed for EG and cannot be detected for 1,2-PG. However, after annealing to 870 K, surface order is restored, and the D<sub>2</sub> yield is also recovered. These results provide additional evidence for the importance of the proper alignment of OD groups of neighboring glycols for D<sub>2</sub> formation. Previous studies have also shown that reactions between two neighboring alcohols are completely suppressed on Ne<sup>+</sup>-sputtered TiO<sub>2</sub>(110).<sup>30</sup>

Since D<sub>2</sub> formation results from a redox reaction that requires transfer of electrons from TiO<sub>2</sub>(110) to the adsorbed glycol molecules, we have investigated the role the availability of subsurface charge plays in the reaction. To this end, saturation coverages of OD-labeled EG (Figure 4a) and 1,2-PG

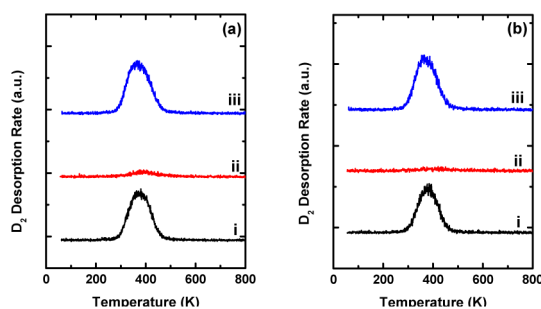


**Figure 3.** Effects of Ne<sup>+</sup> sputtering (~2 ML of Ne<sup>+</sup> at 1.5 kV) of clean TiO<sub>2</sub>(110) on D<sub>2</sub> formation from ethylene (a) and 1,2-propylene (b) glycols. Saturation coverages of OD-labeled EG and 1,2-PG were dosed at 80 K. (i) Ordered TiO<sub>2</sub>(110) before sputtering; (ii) after sputtering; (iii) sputtered and annealed to 870 K.

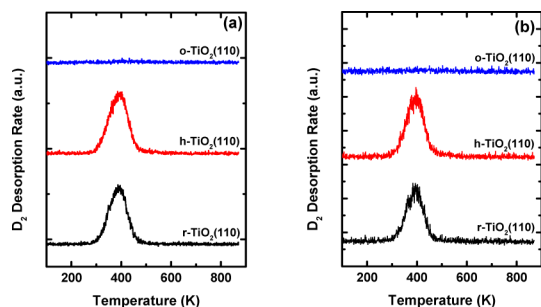


**Figure 4.** TPD spectra of D<sub>2</sub> from ethylene (a) and 1,2-propylene (b) glycols on *r*-, *h*-, and *o*-TiO<sub>2</sub>(110). Saturation coverages of OD-labeled EG and 1,2-PG were dosed at 80 K.

(Figure 4b) were dosed at 80 K on three differently prepared surfaces, i.e., *r*-TiO<sub>2</sub>(110), *h*-TiO<sub>2</sub>(110), and *o*-TiO<sub>2</sub>(110). For both glycols, D<sub>2</sub> TPD peaks from *h*- and *r*-TiO<sub>2</sub>(110) are nearly identical, suggesting that hydroxylation does not influence D<sub>2</sub> formation. Interestingly, on *o*-TiO<sub>2</sub>(110), D<sub>2</sub> formation is completely suppressed for both EG and 1,2-PG.

These results can be interpreted in light of what is known about the effect of surface treatments on the charge state of the TiO<sub>2</sub>(110) surface.<sup>4</sup> Both photoemission spectroscopy<sup>31</sup> and electron energy loss spectroscopy<sup>32</sup> studies have shown that both *r*- and *h*-TiO<sub>2</sub>(110) exhibit essentially the same defect-related electronic states. In contrast, the oxidation of TiO<sub>2</sub>(110) is known to remove these states.<sup>31</sup> Furthermore, in a recent study<sup>27</sup> Petrik *et al.* demonstrated that the amount of charge associated with the surface defects determines the amount of chemisorbed O<sub>2</sub>, and is equivalent on both *r*-TiO<sub>2</sub>(110) and *h*-TiO<sub>2</sub>(110). Similarly, D<sub>2</sub> formation from the glycol OD groups on *r*- and *h*-TiO<sub>2</sub>(110) follows the same trend.

While for *o*-TiO<sub>2</sub>(110), the oxygen adatoms left on Ti<sub>5c</sub> rows<sup>33,34</sup> are expected to serve as a barrier for the formation of glycol pairs, such a small amount (~5%) should not significantly suppress D<sub>2</sub> formation. A more likely origin of the complete suppression of D<sub>2</sub> production stems from the electron scavenging properties of O<sub>a</sub>'s.<sup>2,31,35</sup> As a result, on *o*-TiO<sub>2</sub>(110) the defect electrons become unavailable to adsorbed glycol molecules, preventing the redox reaction leading to D<sub>2</sub>. These results clearly show that subsurface charge is required in D<sub>2</sub> formation.

The chemical insight derived from the glycol studies presented here should be also applicable to alcohol reactions on TiO<sub>2</sub>(110). Surprisingly, hydrogen is generally not

observed<sup>15–18</sup> and/or represents only a minority product.<sup>22</sup> This can be understood upon closer inspection. From Figure 1a, D<sub>2</sub> desorption peaks at ~400 K. For alcohols, the desorption from Ti<sub>5c</sub> sites is usually maximized between 280 and 350 K,<sup>29</sup> at least 50 K lower than the temperature of hydrogen formation. This means that at the temperature of hydrogen formation, most of the alcohol molecules have already desorbed, and only alkoxy species formed by alcohol dissociation on V<sub>O</sub> sites are present. As such, the probability of having two neighboring Ti<sub>5c</sub>-bound alcohol molecules at temperatures required for H<sub>2</sub> formation is negligible. In contrast, the glycol molecules with two hydroxyl groups bind more strongly with TiO<sub>2</sub>(110) and hence desorb at a much higher temperature than alcohols (see Figure S3 in SI). More importantly, the fraction of glycols that desorb intact is small (~20% for EG) as the majority is being converted to products.<sup>23</sup> Therefore, there is sufficient coverage of glycols on TiO<sub>2</sub>(110) at ~400 K for the formation of two neighboring glycol species and D<sub>2</sub>.

In summary, we have shown that molecular hydrogen formation from glycols on TiO<sub>2</sub>(110) is dictated by many factors, that include glycol coverage, steric constraints of glycol molecules, surface order, and the charge state of TiO<sub>2</sub>(110). Hydrogen formation is only observed at high glycol coverages. Increasing the steric hindrance of glycols is found to inhibit and eventually eliminate hydrogen formation. Damaging the surface order or scavenging the available surface charge of TiO<sub>2</sub>(110) are also shown to completely suppress hydrogen formation. These findings provide strong evidence that hydrogen formation results from the bimolecular reaction between two hydroxyl groups of neighboring Ti<sub>5c</sub>-bound glycols, and that the redox reaction is driven by defect electrons of TiO<sub>2</sub>(110).

## ■ ASSOCIATED CONTENT

### ■ Supporting Information

Preparation procedure for OD-labeled glycols; TPD spectra from TiO<sub>2</sub>(110) saturated by commercially available and H/D-exchanged 1,2-PG; TPD spectra of products following 0.06 and 0.57 ML EG dose; TPD spectra of parent glycol molecules; C 1s XPS spectra for glycol saturation coverages; D<sub>2</sub> desorption yields as a function of glycol coverages. This material is available free of charge via the Internet at <http://pubs.acs.org>.

## ■ AUTHOR INFORMATION

### Corresponding Author

zdenek.dohnalek@pnnl.gov

### Present Address

<sup>†</sup>Z.L.: Evans Analytical Group, Sunnyvale, CA

### Notes

The authors declare no competing financial interest.

## ■ ACKNOWLEDGMENTS

We thank R. Rousseau and N. G. Petrik for numerous stimulating discussions. This work was supported by the U.S. Department of Energy, Office of Basic Energy Sciences, Division of Chemical Sciences, Geosciences & Biosciences, and performed in EMSL, a national scientific user facility sponsored by the Department of Energy's Office of Biological and Environmental Research and located at Pacific Northwest National Laboratory (PNNL). PNNL is a multiprogram national laboratory operated for the DOE by Battelle.

## ■ REFERENCES

- (1) Diebold, U. *Surf. Sci. Rep.* **2003**, *48*, 53.
- (2) Henderson, M. A. *Surf. Sci. Rep.* **2011**, *66*, 185.
- (3) Pang, C. L.; Lindsay, R.; Thornton, G. *Chem. Rev.* **2013**, *113*, 3887.
- (4) Dohnálek, Z.; Lyubinetzky, I.; Rousseau, R. *Prog. Surf. Sci.* **2010**, *85*, 161.
- (5) Henderson, M. A.; Lyubinetzky, I. *Chem. Rev.* **2013**, *113*, 4428.
- (6) Chen, X.; Shen, S.; Guo, L.; Mao, S. S. *Chem. Rev.* **2010**, *110*, 6503.
- (7) Ye, M.; Gong, J.; Lai, Y.; Lin, C.; Lin, Z. *J. Am. Chem. Soc.* **2012**, *134*, 15720.
- (8) Khnayzer, R. S.; Thompson, L. B.; Zamkov, M.; Ardo, S.; Meyer, G. J.; Murphy, C. J.; Castellano, F. N. *J. Phys. Chem. C* **2011**, *116*, 1429.
- (9) Wendt, S.; Matthiesen, J.; Schaub, R.; Vestergaard, E. K.; Lægsgaard, E.; Besenbacher, F.; Hammer, B. *Phys. Rev. Lett.* **2006**, *96*, 066107.
- (10) Bikondoa, O.; Pang, C. L.; Ithnin, R.; Murny, C. A.; Onishi, H.; Thornton, G. *Nat. Mater.* **2006**, *5*, 189.
- (11) Zhang, Z.; Bondarchuk, O.; White, J. M.; Kay, B. D.; Dohnálek, Z. *J. Am. Chem. Soc.* **2006**, *128*, 4198.
- (12) Zhang, Z.; Bondarchuk, O.; Kay, B. D.; White, J. M.; Dohnálek, Z. *J. Phys. Chem. C* **2007**, *111*, 3021.
- (13) Zhang, Z.; Rousseau, R.; Gong, J.; Kay, B. D.; Dohnálek, Z. *J. Am. Chem. Soc.* **2009**, *131*, 17926.
- (14) Henderson, M. A. *Langmuir* **1996**, *12*, 5093.
- (15) Henderson, M. A.; Otero-Tapia, S.; Castro, M. E. *Faraday Discuss.* **1999**, *114*, 313.
- (16) Kim, Y. K.; Kay, B. D.; White, J. M.; Dohnálek, Z. *J. Phys. Chem. C* **2007**, *111*, 18236.
- (17) Kim, Y. K.; Kay, B. D.; White, J. M.; Dohnálek, Z. *Surf. Sci.* **2008**, *602*, 511.
- (18) Gamble, L.; Jung, L. S.; Campbell, C. T. *Surf. Sci.* **1996**, *348*, 1.
- (19) Yin, X. L.; Calatayud, M.; Qiu, H.; Wang, Y.; Birkner, A.; Minot, C.; Wöll, C. *ChemPhysChem* **2008**, *9*, 253.
- (20) Kowalski, P. M.; Meyer, B.; Marx, D. *Phys. Rev. B* **2009**, *79*, 115410.
- (21) Du, Y.; Petrik, N. G.; Deskins, N. A.; Wang, Z.; Henderson, M. A.; Kimmel, G. A.; Lyubinetzky, I. *Phys. Chem. Chem. Phys.* **2012**, *14*, 3066.
- (22) Xu, C.; Yang, W.; Guo, Q.; Dai, D.; Chen, M.; Yang, X. *J. Am. Chem. Soc.* **2013**, *135*, 10206.
- (23) Li, Z.; Kay, B. D.; Dohnálek, Z. *Phys. Chem. Chem. Phys.* **2013**, *15*, 12180.
- (24) Farfan-Arribas, E.; Madix, R. J. *J. Phys. Chem. B* **2002**, *106*, 10680.
- (25) Dohnálek, Z.; Kim, J.; Bondarchuk, O.; White, J. M.; Kay, B. D. *J. Phys. Chem. B* **2006**, *110*, 6229.
- (26) Zehr, R. T.; Henderson, M. A. *Surf. Sci.* **2008**, *602*, 1507.
- (27) Petrik, N. G.; Zhang, Z.; Du, Y.; Dohnálek, Z.; Lyubinetzky, I.; Kimmel, G. A. *J. Phys. Chem. C* **2009**, *113*, 12407.
- (28) Kim, B.; Li, Z.; Kay, B. D.; Dohnálek, Z.; Kim, Y. K. *J. Phys. Chem. C* **2012**, *116*, 1145.
- (29) Li, Z.; Smith, R. S.; Kay, B. D.; Dohnálek, Z. *J. Phys. Chem. C* **2011**, *115*, 22534.
- (30) Bondarchuk, O.; Kim, Y. K.; White, J. M.; Kim, J.; Kay, B. D.; Dohnálek, Z. *J. Phys. Chem. C* **2007**, *111*, 11059.
- (31) Wendt, S.; Sprunger, P. T.; Lira, E.; Madsen, G. K. H.; Li, Z.; Hansen, J. Ø.; Matthiesen, J.; Blekinge-Rasmussen, A.; Lægsgaard, E.; Hammer, B.; Besenbacher, F. *Science* **2008**, *320*, 1755.
- (32) Henderson, M. A.; Epling, W. S.; Peden, C. H. F.; Perkins, C. L. *J. Phys. Chem. B* **2003**, *107*, 534.
- (33) Epling, W. S.; Peden, C. H. F.; Henderson, M. A.; Diebold, U. *Surf. Sci.* **1998**, *412–413*, 333.
- (34) Henderson, M. A.; Epling, W. S.; Perkins, C. L.; Peden, C. H. F.; Diebold, U. *J. Phys. Chem. B* **1999**, *103*, 5328.
- (35) Zhang, Z.; Cao, K.; Yates, J. T., Jr. *J. Phys. Chem. Lett.* **2013**, *4*, 674.